DOI: 10.1002/ejic.200501064

Luminescence Modulation of a Terbium Complex with Anions and Its Application as a Reagent

Dengqing Zhang,[a] Mei Shi,[a] Zhiqiang Liu,[a] Fuyou Li,*[a] Tao Yi,[a] and Chunhui Huang*[a]

Keywords: Luminescence modulations / Fluoride anions / Terbium complexes

A terbium complex $Tb(PMIP)_3(PhCN)$, namely tris(1-phenyl-3-methyl-4-isobutyl-5-pyrazolone)-terbium-(pyrazino[2,3-*f*][1,10]phenanthroline-2,3-dicarbonitrile), was synthesized as a reagent for anions. Compared with $Tb(PMIP)_3(H_2O)_2$, the fluorescent quantum yield of $Tb(PMIP)_3(PhCN)$ was reduced because the triplet energy level of PhCN (20920 cm^{-1}) is a little higher than that of $^5D_4$ of Tb^{3+} (20400 cm^{-1}) and lower than that of PMIP (23000 cm^{-1}). This resulted in a back-energy transfer from Tb^{3+} to PhCN. Interestingly, the photoluminescent properties of $Tb(PMIP)_3(PhCN)$ drastically depend on the nature of the anions added into the solution. When apropos equivalents of fluoride (or acetate) anions were added into the CH_3CN solution of $Tb(PMIP)_3(PhCN)$, the replacement of PhCN with fluoride (or acetate) anions took place and the above back-energy transfer was prohibited, which resulted in a fluorescence enhancement of the terbium complex. After excessive equivalents of fluoride (or acetate) anions were added, the replacement of PMIP with fluoride (or acetate) anions prohibited the ligand PMIP sensitized energy transfer of the terbium complex, resulting in the fluorescence quenching of the system. However, in the aqueous solution, the terbium complex shows a remarkable selectivity of fluoride anions over the other anions. As a reagent, its sensitivity is about 10^{-8} mol·L^{-1} for the fluoride anions.

Introduction

Anion recognition and sensing are of current interest because of their importance in biological, environmental, and chemical systems.[1–4] The construction of anion chemosensors is essentially composed of two units, the binding site and the signaling subunit, which may be covalently linked (binding site-signaling submit approach)[5–8] or not (displacement approach).[9] The interaction with the anion and the change in color or fluorescence are in principle reversible. However, development of fluorescent reagents has emerged as a research area of significant importance.[1,10,11] In these systems, anion signaling using fluorescence or color changes can also be observed using irreversible reactions.[12] The underlying idea of these irreversible systems is to take advantage of the selective reactivity that certain anions may display. Hence, the use of an anion-induced reagent system usually has high selectivity and also an accumulative effect is directly related with the anion concentration. Fluoride, the smallest anion, has unique biological and chemical properties, and its recognition and detection are of growing interest because it is associated with dental care[13] and the treatment of osteoporosis.[14] As a result, there is a need to develop new sensitive methods for fluoride detection. Most of the emerging detection methods have focused on the specific Lewis acid-base interaction, such as the strong affinity of a boron atom towards the fluoride anion,[15–19] or the designed hydrogen bonding with the fluoride anion.[20,21] These binding events have been converted into an electrochemical[22] or fluorescent change,[23–26] or more directly, colorimetric change seen by the naked eye.[27,28] However, the reported fluorescent reagents for fluoride anions is quite limited.[29–31]

In the past decade, the synthesis, characterization, and application of luminescent lanthanide complexes have been the focus of much attention.[32–35] On the basis of the unique photophysical properties of lanthanide cations (long luminescence lifetime and very sharp emission band),[36,37] lanthanide complexes as luminescent materials were paid particular attention in the immunoassay[38] and organic light-emitting diode (OLED).[39–42] Recently, some luminescent lanthanide complexes have been used as a chemosensor for anions.[43–50] For example, Ziessel et al. reported that several lanthanide complexes were engineered from a ligand consisting of a single P=O fragment and two methylene linked bipyridine subunits for nitrate anion detection.[49,50] It is well known that fluoride anions bind tightly with lanthanide ions, and some work has reported on the influence of fluoride anions on the luminescence property of crown-based lanthanide complexes by exchanging coordinated water with fluoride anions.[51,52] In this paper, a new terbium complex $Tb(PMIP)_3(PhCN)$ (see Scheme 1) was designed and synthesized as a reagent for detecting anions by another mechanism. Here, PMIP and PhCN stand for

[a] Laboratory of Advanced Materials, Fudan University, Shanghai, 200433, P. R. China

the anion of 4-isobutyl-3-methyl-1-phenyl-5-pyrazolone and pyrazino[2,3-*f*][1,10]phenanthroline-2,3-dicarbonitrile, respectively. The photophysical studies of $Tb(PMIP)_3(PhCN)$ showed that the luminescent properties of this complex could be modulated upon addition of the different anions.

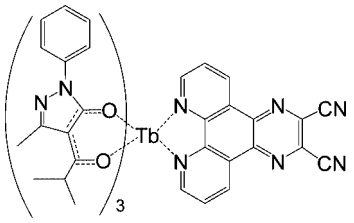

Scheme 1. Chemical structure of $Tb(PMIP)_3(PhCN)$.

Results and Discussion

Structure Characterization of $Gd(PMIP)_3(H_2O)_2$·$Gd(PMIP)_3(C_2H_5OH)(H_2O)$ (A)

The structure of the gadolinium complex **A** was characterized by X-ray crystallography. An ORTEP diagram for the asymmetric unit is shown in Figure 1. Details of the crystal data and data collection parameters for **A** are given in Table 1. It can be seen form Figure 1 that a common repeating unit exists for the two molecules of $Gd(PMIP)_3(H_2O)_2$ and $Gd(PMIP)_3(C_2H_5OH)(H_2O)$. In $Gd(PMIP)_3(H_2O)_2$, the geometry around the central ions can be described as a distorted bicapped-trigonal prism where the trigonal prism is composed of six oxygen atoms (O9, O10, O12, O13, O15, O16). Among them, O9 and O10 are from one β-diketone, O12 and O13 are from the other two β-diketones, and O15 and O16 are from two water molecules. Another two oxygen atoms (O11, O14) cap the two quadrilateral faces O9–O10–O12–O16 and O9–O15–O13–O16, respectively. The average Gd–O distance is 2.42 Å [2.31(2)–2.53(3)], which is a little smaller than the sum of the radii of Gd^{3+} (1.05 Å, eight coordinated) and O^{2-} (1.42 Å). Furthermore, the structure of $Gd(PMIP)_3(C_2H_5OH)(H_2O)$ is the same as that of $Gd(PMIP)_3(H_2O)_2$ except for an ethanol molecule occurring in place of the water molecule, the coordination geometry is that of distorted a bicapped-trigo-

Table 1. Crystal data, collection and structure refinement parameters for complex **A**.

	$Gd(PMIP)_3(H_2O)_2Gd(PMIP)_3(C_2H_5OH)(H_2O)$
Empirical formula	$C_{87}H_{108}Gd_2N_{12}O_{18}$
M_r [g mol^{-1}]	1924.35
Crystal system	triclinic
Space group	$P\bar{1}$
Crystal size [mm]	0.40 × 0.25 × 0.18
a [Å]	13.2931(2)
b [Å]	18.0432(2)
c [Å]	18.7608(3)
α [°]	77.3215(5)
β [°]	86.4151(5)
γ [°]	89.7183(7)
V [Å^3]	4381.29(11)
Z	2
$\rho_{calcd.}$ [g cm^{-3}]	1.459
μ [mm^{-1}]	1.574
F (000)	1972
R_1 [$I > 2\sigma(I)$]	0.0422
wR_2 [$I > 2\sigma(I)$]	0.0684
R_1 (all data)	0.1134
wR_2 (all data)	0.0826
GOF	0.938

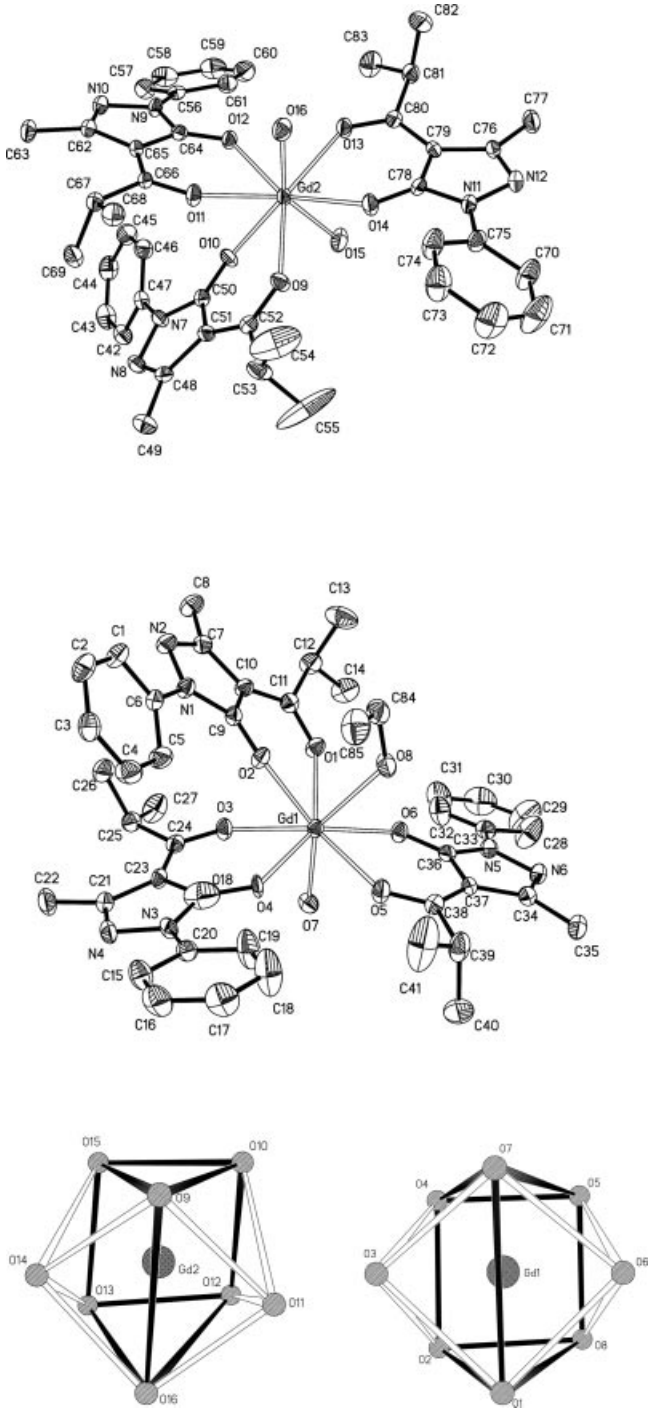

Figure 1. ORTEP diagram of **A** with the thermal ellipsoids drawn at the 30% probability level and the H atoms removed for clarity.

nal prism, as illustrated in Figure 1. Moreover, an independent C_2H_5OH solvent molecule exists in the unit cell.

UV/Vis Spectra

UV/Vis absorption spectra of the ligands (PMIP and PhCN) and $Tb(PMIP)_3(PhCN)$ in CH_3CN solution are shown in Figure 2. The maximum absorption band of PMIP at 263 nm is attributed to a singlet-singlet π-π* enol absorption of the β-diketonate. The ligand PhCN has two absorption bands at 264 and 306 nm, which are attributed to n-π* and singlet-singlet π-π* absorption, respectively. Compared with the spectrum of PMIP, the absorption maximum of $Tb(PMIP)_3(PhCN)$ is red-shifted by 5 nm, which is agreement with the enlargement of the conjugated structure of ligands after coordinating to the terbium ion. It can be seen from Figure 2 that the spectral shape of $Tb(PMIP)_3(PhCN)$ in CH_3CN is similar to that of PMIP, indicating that the coordination of the terbium ion does not significantly influence the singlet-state energy of PMIP. The molar absorption coefficients (ε) of PMIP, PhCN, and $Tb(PMIP)_3(PhCN)$ are calculated as 2.55×10^4, 6.11×10^4, and 9.61×10^4 $L\cdot mol^{-1}\cdot cm^{-1}$, respectively, revealing that the two ligands and the terbium complex have a strong ability to absorb light.

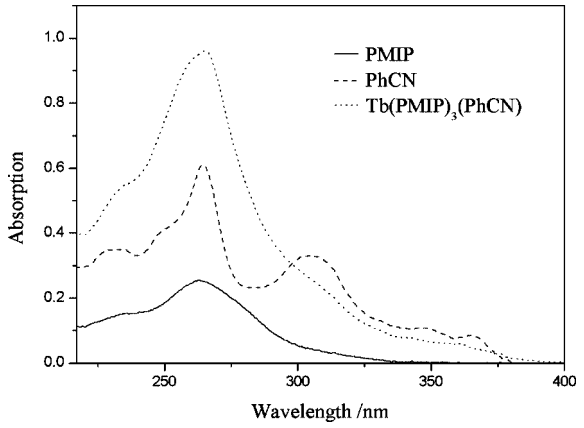

Figure 2. UV/Vis spectra of PMIP, PhCN, and $Tb(PMIP)_3(PhCN)$ in CH_3CN (1.0×10^{-5} $mol\cdot L^{-1}$).

Fluorescence Characteristics

The fluorescence spectrum of $Tb(PMIP)_3(PhCN)$ in CH_3CN solution (see Figure 3) shows characteristic emission bands of Tb^{3+} (λ_{ex} = 280 nm) centered at 489, 544, 584, and 612 nm resulting from the deactivation of the $^5D_4$ excited state to the corresponding ground state ^7F_J (J = 6, 5, 4, 3) of the Tb^{3+} ion. The strongest emission is centered around 544 nm and corresponds to the hypersensitive transition of $^5D_4\rightarrow{}^7F_5$. The excitation spectrum of $Tb(PMIP)_3$-(PhCN) overlays the absorption wavelength range of PMIP well, indicating that the emission of $Tb(PMIP)_3(PhCN)$ originates mainly from the energy absorbed by PMIP. We also investigated the emission spectrum of $Tb(PMIP)_3$-(PhCN) in the different solvents, such as $CHCl_3$, DMF, and DMSO, the similarity of the emission patterns in these solvents suggests that there are no solvent-dependent structural changes.

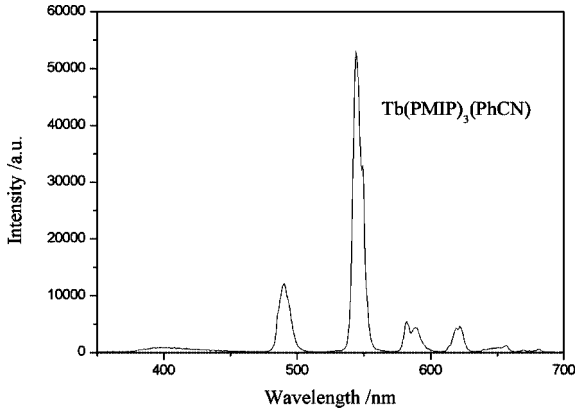

Figure 3. The luminescence spectrum of $Tb(PMIP)_3(PhCN)$ at 298 K in CH_3CN.

Phosphorescence Spectra

Since the first excited energy level of the Gd^{3+} ion ($^6P_{7/2}$) is high, the energy absorbed by the ligand in the Gd^{3+} complex usually cannot be transferred to the Gd^{3+} ion. Therefore the phosphorescence emission from the Gd^{3+} complex can be considered as ligand-localized phosphorescence emission, and then the energy level of ^{3}π-π* of the ligand can be deduced. At room temperature, the phosphorescent emission spectrum of the Gd^{3+} complex is very weak, however at a lower temperature (77 K), the ligand-localized phosphorescent spectrum can be observed. Herein, the gadolinium complexes $Gd(NO_3)_3(PhCN)$ and **A** were synthesized for triplet-energy level measurements. The phosphorescent spectra of **A** and $Gd(NO_3)_3(PhCN)$ at 77 K are shown in Figure 4. The emission bands of **A** and $Gd(NO_3)_3(PhCN)$ peak at 464 nm (21552 cm^{-1}) and 502 nm (19920 cm^{-1}), respectively. By referring to the lower wavelength emission edges of the corresponding phosphorescent

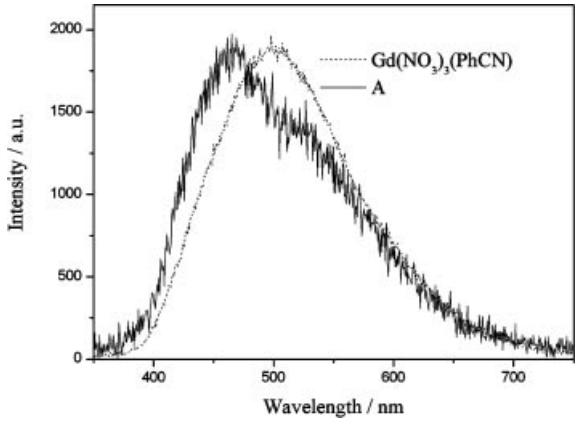

Figure 4. Phosphorescent spectra of **A** and $Gd(NO_3)_3(PhCN)$ at 77 K.

spectra, the energies of zero-phonon transition of the triplet states ($^3\pi\pi^*$) at about 435 nm (23000 cm^{-1}) and 478 nm (20920 cm^{-1}) were obtained for PMIP and PhCN, respectively.

Photophysical Properties of the Terbium Complexes

By using Rhodamine 6G in ethanol (1×10^{-6} mol·L^{-1}, φ_{ref} = 0.92) as a reference, the overall luminescence quantum yields ($\varphi_{overall}$) of $Tb(PMIP)_3(PhCN)$ and $Tb(PMIP)_3(H_2O)_2$ in CH_3CN were measured to be 0.15% and 2.97% according to the well-known method.[53] The luminescence lifetimes (τ) were also investigated for $Tb(PMIP)_3(PhCN)$ and $Tb(PMIP)_3(H_2O)_2$ in CH_3CN. The measured luminescent decay can be described by monoexponential kinetics, and the luminescence lifetimes of $Tb(PMIP)_3(PhCN)$ and $Tb(PMIP)_3(H_2O)_2$ are 95.5 and 341.1 μs, respectively.

In order to understand the influence of the ligand modification on the photophysical property of $Tb(PMIP)_3(PhCN)$, the efficiency of energy transfer ($\varphi_{transfer}$) from the ligand to Tb^{3+} and the probability of the terbium emission (φ_{Ln}) were investigated for $Tb(PMIP)_3(PhCN)$ and $Tb(PMIP)_3(H_2O)_2$ on the basis of the method developed by Selvin et al.[54] The overall quantum yield ($\varphi_{overall}$) can be defined as Equation (1).

$$\varphi_{overall} = \varphi_{transfer}\varphi_{Ln} \quad (1)$$

When a lanthanide complex is mixed with an acceptor of known quantum yield and very short fluorescence lifetime (ns), the efficiency of energy transfer between them (φ_{ET}) and the probability of lanthanide emission (φ_{Ln}) are calculated from both the fluorescence decay lifetime and intensity measurements, see Equation(2) and (3).

$$\varphi_{ET} = 1 - (\tau_{da}/\tau_d) \quad (2)$$

$$\varphi_{Ln} = \varphi_a(I_{da}/I_{ad})/(1/\varphi_{ET} - 1) = \varphi_a I_{da}(\tau_d - \tau_{ad})/(I_{ad}\tau_{ad}) \quad (3)$$

Here τ_{ad} and τ_d are the excited state lifetime of the lanthanide complex in the presence and absence of the acceptor, respectively; φ_a is the fluorescence quantum yield of the acceptor; I_{da} is the integral area under the residual lanthanide emission in the presence of the acceptor; and I_{ad} is the integral area of the fluorescent emission part of the acceptor.

Here, Rhodamine 6G was used as the acceptor in ethanol (φ_a = 0.92 and $\tau < 10$ ns). For example, in a mixture solution consisting of $Tb(PMIP)_3(PhCN)$ (10 μM) and Rhodamine 6G (1.25 μM), the emission lifetime of the Tb^{III} complex (λ_{em} = 544 nm) decreased from 95.5 to 80.0 μs, indicating that 16.2% of the energy was transferred from $Tb(PMIP)_3(PhCN)$ to Rhodamine 6G. From these measurements and Equation (3), the probability of Tb^{3+} emission (φ_{Ln}) in $Tb(PMIP)_3(PhCN)$ was determined to be 1.1% (Table 2). In combination with the overall quantum yield ($\varphi_{overall}$) of $Tb(PMIP)_3(PhCN)$, the efficiency of energy transfer ($\varphi_{transfer}$) from the ligand to Tb^{3+} was calculated to be 14.2% (see Table 2) according to Equation (1). Similarly, the efficiency of energy transfer ($\varphi_{transfer}$) of 56.3% and the probability of Tb^{3+} emission (φ_{Ln}) of 5.3% were obtained for $Tb(PMIP)_3(H_2O)_2$.

With φ_{Ln} and τ_d determined in acetonitrile, radiative and nonradiative decay rates of the Tb^{III} complex were calculated from Equation (4).

$$k_{rad} = \varphi_{Ln}/\tau_d k_{nr} = (1 - \varphi_{Ln})/\tau_d \quad (4)$$

Taking 1.1% of φ_{Ln} and 95.5 μs of τ_d into account, the radiative and norradiative decay rates of $Tb(PMIP)_3(PhCN)$ were calculated as 111 and 1.04×10^4 s^{-1}, respectively (see Table 2). Similarly, the radiative and nonradiative decay rates of $Tb(PMIP)_3(H_2O)_2$ were determined as 151 and 2.71×10^3 s^{-1} (see Table 2), respectively.

To elucidate the energy transfer process of the terbium complex, the energy levels of the relevant electronic states should be estimated. By referring to their wavelengths at the UV/Vis absorbance edges, the singlet-energy levels of PMIP and PhCN were estimated to be 32260 cm^{-1} (310 nm) and 29410 cm^{-1} (340 nm), respectively. In combination with the triplet-energy levels of PMIP and PhCN, the schematic energy level diagram and the energy transfer process are shown in Figure 5.

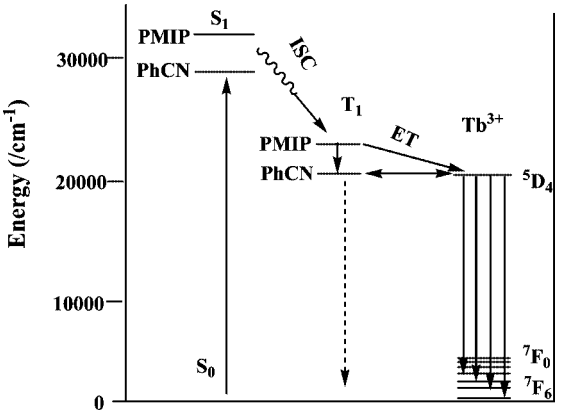

Figure 5. Schematic energy level diagram and the energy transfer process in the system of $Tb(PMIP)_3(PhCN)$. S_1: the first excited singlet state, T_1: the first excited triplet state.

Generally, the sensitization pathway in luminescent terbium complexes consists of the excitation of the ligands from the ground state to their excited singlet states, and

Table 2. Photophyscical properties of $Tb(PMIP)_3(PhCN)$ and $Tb(PMIP)_3(H_2O)_2$ in CH_3CN.

System	λ_{max}^{PL} [nm]	τ [μs]	$\varphi_{overall}$ [$\times10^3$]	φ_{Ln} [%]	$\varphi_{transfer}$ [%]	k_{rad} [s^{-1}]	k_{nr} [s^{-1}]
$Tb(PMIP)_3(H_2O)_2$	544	341.1	29.7	5.3	56.3	151	2.71×10^3
$Tb(PMIP)_3(PhCN)$	544	95.5	1.5	1.1	14.2	111	1.04×10^4
$Tb(PMIP)_3(PhCN) + 3F^-$	544	114.9	10.5	3.7	28.4	321	8.4×10^3

subsequently through the intersystem crossing of the ligands to their triplet states, following the energy transfer from the triplet state of the ligand to the central ion. In this process the 4f electrons of the Tb^{3+} ion are excited to the ^5D_J manifold ion from the ground state, finally the Tb^{3+} ion emits when the 4f electrons undergo a transition from the excited state of $^5D_4$ to the ground state.[55,56] We noticed that the energy gaps ΔE ($^1\pi\pi^*$-$^3\pi\pi^*$) between the $^1\pi\pi^*$ and $^3\pi\pi^*$ levels are 9260 and 8490 cm^{-1} for PMIP and PhCN, respectively (see Figure 5). According to Reinhoudt's empirical rule that the intersystem crossing process will be effective when ΔE ($^1\pi\pi^*$-$^3\pi\pi^*$) is at least 5000 cm^{-1},[57] the intersystem crossing processes are effective for PMIP and PhCN. On the other hand, the triplet-energy level of PMIP ($\approx$23000 cm^{-1}) is higher than that of $^5D_4$ (20400 cm^{-1}) for Tb^{3+}, and their energy gap ΔE ($^3\pi\pi^*$-$^5D_4$) between the ligand- and metal-centered level is 2600 cm^{-1}. According to Latva's empirical rule,[58] an optimal ligand-to-metal transfer process for Tb^{III} is when ΔE ($^3\pi\pi^*$-$^5D_0$) > 2000 cm^{-1}. It can be concluded that the transfer process is also effective from PMIP to Tb^{3+} and that PMIP is suitable as a sensitizer for Tb^{III}. On the contrary, the $^3\pi\pi^*$ state (ca. 20920 cm^{-1}) of PhCN is so close to $^5D_4$ (20400 cm^{-1}) of Tb^{3+}, giving ΔE ($^3\pi\pi^*$-$^5D_0$) = 520 cm^{-1}, which is too low to prevent the back-energy transfer from the Tb^{3+} excited state to the triplet state of PhCN. Moreover, the triplet energy level of PhCN is lower than that of PMIP, and the energy transfer from PMIP to PhCN may occur. Therefore, it is not difficult to understand the fact that $Tb(PMIP)_3(PhCN)$ exhibits a lower fluorescence quantum yield ($\varphi_{overall}$) (0.15%) compared to that (2.97%) of $Tb(PMIP)_3(H_2O)$.

Fluorescence Modulation of the Complex with Anions

The fluorescence modulation of $Tb(PMIP)_3(PhCN)$ with anions was investigated by the fluorescence titration experiments in CH_3CN. Figure 6 shows the titration curves of the spectral parameters of $Tb(PMIP)_3(PhCN)$ against the [anion]/[$Tb(PMIP)_3(PhCN)$] ratio in acetonitrile. Interestingly, a different fluorescent modulation of $Tb(PMIP)_3$-(PhCN) was observed upon addition of the different anions. For example, a slight variation of the luminescent properties of $Tb(PMIP)_3(PhCN)$ was observed upon addition of other anions such as ClO_4^-, NO_3^-, or NO_2^-. When one equivalent of Cl^-, Br^-, or I^- was added, the fluorescent intensity of $Tb(PMIP)_3(PhCN)$ reached the maximum (see Figure 6), and then it was almost unchanged with further addition of Cl^-, Br^-, or I^-. Similarly, Mahajan et al. reported that the luminescence intensity of tris(β-diketonate) europium (λ_{em} = 611 nm) was enhanced twofold when three equivalents of Cl^- were added.[47] Generally, the coordination number of the Tb^{III} complexes in solution is nine.[59] The coordination number of Tb^{3+} in $Tb(PMIP)_3(PhCN)$ is eight, implying that the complex can bond one anion to form a coordination of nine, hence, the increasing fluorescent emission was observed upon addition of one equivalent of the anions. Because of their weak bonding ability to the terbium ion, Cl^-, Br^-, and I^- had difficultly in displacing the ligands PhCN and PMIP, which was confirmed by the fact that there was no obvious change in the luminescent emission of $Tb(PMIP)_3(PhCN)$ with further addition of Cl^-, Br^-, or I^- (see Figure 6).

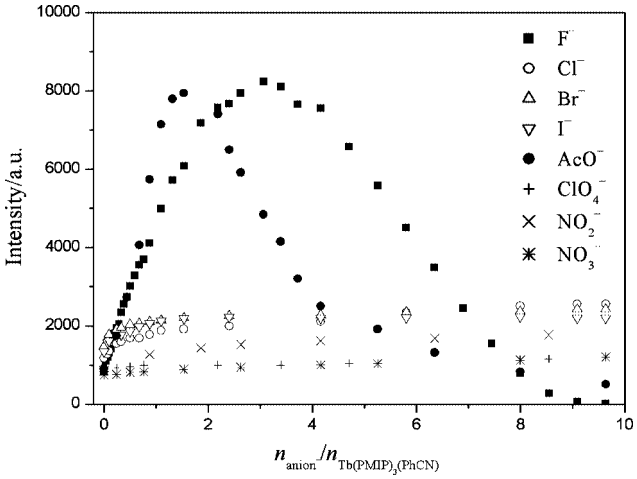

Figure 6. Fluorescent titrations of $Tb(PMIP)_3(PhCN)$ (1.0×10^{-5} mol·L^{-1}) in CH_3CN upon addition of F^-, Cl^-, Br^-, I^-, ClO_4^-, NO_3^-, NO_2^-, and AcO^-.

It is well known that the lanthanide complex receptor prefers smaller (harder) F^- (or AcO^-) to larger (softer) Cl^-, Br^-, or I^-. In fact, a special fluorescent modulation of $Tb(PMIP)_3(PhCN)$ was observed upon addition of fluoride and acetate anions. For example, Figure 7 shows fluorescent spectral changes of $Tb(PMIP)_3(PhCN)$ in CH_3CN solution (10 μM) upon addition of tetra-*n*-butylammonium fluoride (Bu_4NF). Upon addition of the fluoride anion, the characteristic terbium emission (λ_{ex} = 280 nm) greatly increased along with an increase of the emission intensity of PhCN centred at 400 nm (see Figure 7, a). When Bu_4NF reached about three equivalents of $Tb(PMIP)_3(PhCN)$ (see Figure 7, a), this change became saturated with a fluorescent quantum yield of 1.05%. Under these conditions, the efficiency of energy transfer ($\varphi_{transfer}$) and the probability of Tb^{3+} emission (φ_{Ln}) for this mixture were measured to be 28.4% and 3.7%, respectively (see Table 2). It can be seen from Table 2 that the mixture exhibited a higher energy transfer efficiency ($\varphi_{transfer}$) and larger probability of Tb^{3+} emission compared with $Tb(PMIP)_3(PhCN)$. Because of its strong bonding ability, the fluoride anions were able to substitute one solvent molecule and one PhCN molecule that were weakly coordinated to Tb^{III} in the complex, and so Tb^{III} reached a coordination number of nine, revealing that the back-energy transfer from $^5D_4$ of Tb^{3+} and the triplet state of PMIP to the triplet state of PhCN was restrained (see Figure 5); consequently, both the probability of Tb^{3+} emission (φ_{Ln}) and the fluorescent quantum yield of the mixture were improved. However, further addition of a large excess of Bu_4NF caused a decrease of the characteristic fluorescent emission of Tb^{3+}, and the emission was quenched completely when nine equivalents of Bu_4NF were added (see Figure 7b). These changes can be interpreted as the follow-

ing: upon addition of more fluoride anions, PMIP ligands were completely replaced by fluoride anions, resulting in the breakage of the ligand-sensitized energy transfer from PMIP to Tb^{3+}, consequently reducing the fluorescent quantum yield of the complex. Compared with the fluoride anion, the acetate anion exhibited a similar modulation behavior for the fluorescent emission of the terbium complex (see Figure 6). From the above results, we can see that the addition of fluoride and acetate anions affects the quantum yield of Tb^{3+} emission and modulates the energy transfer path, which finally results in the modulation of the overall emission quantum yield.

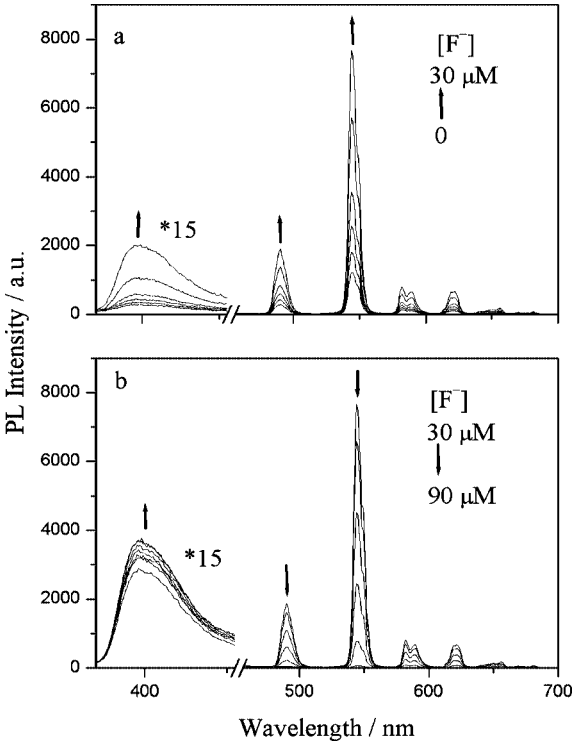

Figure 7. Fluorescent titrations of $Tb(PMIP)_3(PhCN)$ (1.0×10^{-5} mol·L^{-1}) upon addition of Bu_4NF.

However, when $Tb(PMIP)_3(PhCN)$ was dissolved in the mixture of CH_3CN/H_2O (9:1 v/v), only a decrease in fluorescent emission of the complex was observed upon addition of fluoride and acetate anions. Under these conditions, the coordinating water molecules can compete with PhCN fragments and gradually remove them from the first coordination sphere of Tb^{3+}, then back-energy transfer from the Tb^{3+} excited state to the triplet state of PhCN was broken. In fact, the complex exhibited more intense fluorescent emission (φ = 0.62%) in CH_3CN/H_2O (9:1 v/v). When further fluoride anions were added, PMIP was replaced by fluoride anions, resulting in the breakage of the ligand-sensitized energy transfer from PMIP to Tb^{3+} (see Figure 5), and then the fluorescence of Tb^{3+} was quenched. However, fluorescent quenching to different degrees was observed for $Tb(PMIP)_3(PhCN)$ upon addition of the different anions (see Figure 8). Consequently, the complex showed a remarkable selectivity of fluoride anions over the other anions, which may be explained by the small size, the high surface charge density of the fluoride anion and its strong affinity to Tb^{3+}.[60] Even in this situation, the solution is very clear and transparent, the observable sensitivity is about 10^{-8} mol·L^{-1} of fluoride anions.

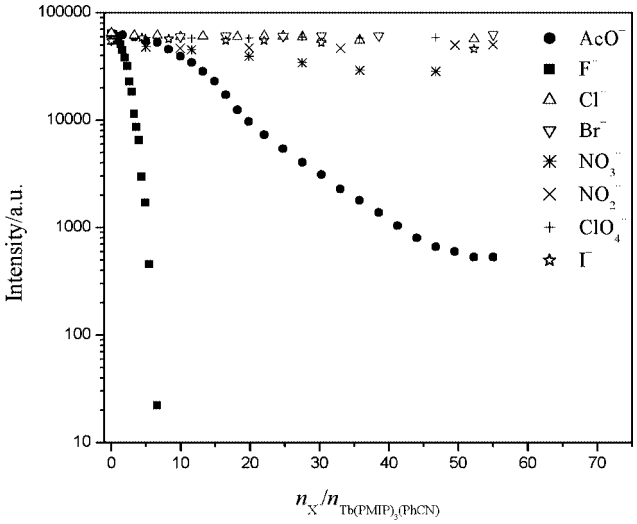

Figure 8. Fluorescent titrations of $Tb(PMIP)_3(PhCN)$ (1.0×10^{-5} mol·L^{-1}) in CH_3CN/H_2O (9:1 v/v) upon addition of F^-, Cl^-, Br^-, I^-, ClO_4^-, NO_3^-, NO_2^-, and AcO^-.

Conclusions

In summary, we have designed and synthesized a novel lanthanide-based luminescent reagent $Tb(PMIP)_3(PhCN)$ for anions. By using Tb^{3+} as the fluorophore, $Tb(PMIP)_3$-(PhCN) displays high selective fluorescent modulation on the fluoride and acetate anions in acetonitrile. The large fluorescent enhancement at first and then fluorescence quenching were observed for the terbium complex upon addition of fluoride and acetate anions. However, in aqueous solution, $Tb(PMIP)_3(PhCN)$ shows a unique fluorescent quenching upon addition of fluoride, indicating its remarkable selectivity for fluoride anions over the other anions. At the same time, the reason for the fluorescence modulation with the anions was described. This system is particularly useful relative to other molecules because it allows detection of traces of fluoride and acetate anions by luminescence monitoring at a terbium center.

Experimental Section

General: Diaminomaleonitrile and tetrabutylammonium fluoride trihydrate were obtained from Acros. $TbCl_3\cdot6H_2O$, $Gd(NO_3)_3\cdot6H_2O$, and 1-phenyl-3-methyl-4-isobutyl-5-pyrazolone were purchased from Shanghai Sinopharm Chemical Reagent Co. Ltd., Phenanthroline-5,6-dione was synthesized according to the literature.[61] The complexes $Tb(PMIP)_3(H_2O)_2$ and $Gd(PMIP)_3(H_2O)_2\cdot Gd(PMIP)_3(C_2H_5OH)(H_2O)$ (**A**) were synthesized according to a similar method reported previously[62] and characterized by elemental analyses. Moreover, the structure of the complex **A** was characterized by X-ray crystallography. UV/Visible absorption

spectra were recorded with a UV 2550 spectrophotometer of Shimadzu. The element analyses were performed with Vario EL III O-Element analyzer. ^{1}HNMR spectra were recorded with a Mercury Plus 400NB NMR spectrometer. The luminescence and phosphorescence spectra were measured with an Edinburgh LFS920 fluorescence spectrophotometer and LP-920 laser flash photolysis spectrophotometer, respectively. For the phosphorescence measurements, the fourth harmonic 266 nm of the pulsed GCR-4 Nd:YAG Laser (Spectra-Physics, USA) with 30 Hz repetition rate and 6 ns pulse width was used as the excitation source, and the experiments were completed at 77 K in ethanol/methanol (1:1 v/v). Fluorescence lifetimes were recorded with a single photon counting spectrometer from Edinburgh LFS920 fluorescence spectrophotometer with microsecond pulse lamp as the excitation source. The data were analyzed by an iterative convolution of the luminescence decay profile with the instrument response function using a software package provided by Edinburgh Instruments.

Synthesis of Pyrazino[2,3-*f*][1,10]phenanthroline-2,3-dicarbonitrile (PhCN): PhCN was synthesized according to a similar method reported previously.[63] 2,3-Diaminomaleonitrile (6.0 mmol) was added to a solution consisting of 1,10-phenanthroline-5,6-dione (1.0 g, 4.8 mmol) and absolute ethanol (30 mL) in a 50 mL flask. The reaction mixture was refluxed for 3 h and then cooled to room temperature. The solution was concentrated to ca. 10 mL with a rotary evaporator and the solid product was filtered. After recrystallization from ethanol twice, the desired pale yellow powder (1.0 g) was obtained with a yield of 74%. ^{1}HNMR (400 MHz, $CDCl_3$): δ = 7.93 (q, 2 H), 9.4–9.46 (d, 2 H), 9.46–9.52 (d, 2 H) ppm. $C_{16}H_6N_6$(282.26): calcd. C 68.08, H 2.14, N 29.77; found C 68.00, H 2.10, N 30.02.

Synthesis of Tb(PMIP)$_3$(PhCN) and Gd(NO$_3$)$_3$(PhCN): The complexes Tb(PMIP)$_3$(PhCN) and Gd(NO$_3$)$_3$(PhCN) were synthesized according to a previous literature procedure.[64]

Tb(PMIP)$_3$(PhCN): Ethanol (10 mL), 4-isobutyl-3-methyl-1-phenyl-5-pyrazolone (3.0 mmol), and triethylamine (3 mmol) were added to a 25 mL side-arm flask. The mixture was stirred for 10 minutes, and then PhCN and $TbCl_3{\cdot}6H_2O$ (1.0 mmol) were added to the flask. The reaction mixture was refluxed for 3 h whilst stirring, and then cooled to room temperature. The solvent was removed under reduced pressure and the residue was washed with water. The crude product was then recrystallized from an ethanol/water mixture (8:2 v/v) to afford the desired product (1.42 g) with a yield of 80%. $C_{58}H_{51}N_{12}O_6Tb$ (1771.03): calcd. C 59.49, H 4.39, N 14.35; found C 59.30, H 4.41, N 14.19.

Gd(NO$_3$)$_3$(PhCN): $Gd(NO_3)_3{\cdot}6H_2O$ (0.25 mmol) was added dropwise whilst stirring to an ethanol solution (10 mL) containing PhCN (0.25 mmol), and then the reaction mixture was refluxed for 4 h. The resulting solution was filtered and a white powder was obtained by recrystallization from an ethanol solution, 117 mg, yield 75%. $C_{16}H_6N_9O_9Gd$ (625.52): calcd. C 30.72, H 0.97, N 20.15; found C 30.65, H 0.91, N 20.10.

Crystallography: The crystal of complex **A** was mounted on a glass fiber and transferred to a Bruker SMART CCD area detector. Crystallographic measurements were carried out using a Bruker Apex II CCD diffractometer, σ scans, graphite-monochromated Mo-K_a radiation (λ = 0.71073 Å) under room temperature. The structures were solved by direct methods and refined by full-matrix least-squares on F^2 values using the program SHELXS-97.[65] All non-hydrogen atoms were refined anisotropically. Hydrogen atoms were calculated in ideal geometries. For the full-matrix least-squares refinements [$I > 2\sigma(I)$], the unweighted and weighted agreement factors of $R_1 = \Sigma(F_o - F_c)/\Sigma F_o$ and $wR_2 = [\Sigma w(F_o^2 - F_c^2)^2/\Sigma wF_o^4]^{1/2}$ were used. The crystal data and details of the structure determinations are summarized in Table 1.

CCDC-288368 contains the supplementary crystallographic data for this paper. These data can be obtained free of charge from The Cambridge Crystallographic Data Centre via www.ccdc.cam.ac.uk/data_request/cif.

Fluorescence Modulation: Fluorescence modulations were carried out in the following manner: the solution of Tb(PMIP)$_3$(PhCN) in a 1.0 cm quartz cuvette was titrated with the concentrated solutions of tetrabutylammonium salts of different anions (X = F^-, Cl^-, Br^-, I^-, ClO_4^-, NO_3^-, NO_2^-, and AcO^-) by a micro sample injector. In order to account for the dilution effect, the volume of these concentrated solutions was negligible. The concentration of Tb(PMIP)$_3$(PhCN) in all experiments was 1.0×10^{-5} mol·L^{-1}.

Acknowledgments

The authors thank the National Science Foundation of China (Grant 20490210 and 20501006), National Basic Research 973 Program (2006CB601103), Shanghai Sci. Tech. Comm. (05DJ14004), and China Postdoctoral Science Foundation for financial support.

[1] R. Martínez-Máñez, F. Sancenón, *Chem. Rev.* **2003**, *103*, 4419–4476.
[2] P. D. Beer, P. A. Gale, *Angew. Chem. Int. Ed.* **2001**, *40*, 486–516.
[3] C. Suksai, T. Tuntulani, *Chem. Soc. Rev.* **2003**, *32*, 192–202.
[4] T. Gunnlaugsson, J. P. Leonard, *Chem. Commun.* **2005**, 3114–3131.
[5] R. A. Bissell, P. de Silva, H. Q. N. Gunaratne, P. L. M. Lynch, G. E. M. Maguire, K. R. A. S. Sandanayake, *Chem. Soc. Rev.* **1992**, *21*, 187–195.
[6] D. Parker, J. H. Yu, *Chem. Commun.* **2005**, 3141–3143.
[7] R. S. Dickins, T. Gunnlaugsson, D. Parker, R. D. Peacock, *Chem. Commun.* **1998**, 1643–1644.
[8] T. Gunnlaugsson, J. P. Leonard, K. Sénéchal, A. J. Harte, *J. Am. Chem. Soc.* **2003**, *125*, 12062–12063.
[9] S. L. Wiskur, H. Ait-Haddou, J. J. Lavigne, E. V. Anslyn, *Acc. Chem. Res.* **2001**, *34*, 963–972.
[10] A. P. de Silva, H. Q. N. Gunaratne, T. Gunnlaugsson, A. J. M. Huxley, C. P. McCoy, J. T. Rademacher, T. E. Rice, *Chem. Rev.* **1997**, *97*, 1515–1566.
[11] B. Liu, H. Tian, *Chem. Commun.* **2005**, 3156–3158.
[12] J. V. Ros-Lis, M. D. Marcos, R. Martínez-Máñez, K. Rurack, J. Soto, *Angew. Chem. Int. Ed.* **2005**, *44*, 4405–4407 and references cited therein.
[13] K. L. Kirk, *Biochemistry of the Halogens and Inorganic Halides*, Plenum Press, New York, **1991**, 58.
[14] M. Kleerekoper, *Endocrinol. Metab. Clin. North Am.* **1998**, *27*, 441.
[15] S. Yamaguchi, S. Akiyama, K. Tamao, *J. Am. Chem. Soc.* **2001**, *123*, 11372–11375.
[16] Y. Kubo, M. Yamamoto, M. Ikeda, M. Takeuchi, S. Shinkai, S. Yamaguchi, K. Tamao, *Angew. Chem. Int. Ed.* **2003**, *42*, 2036–2040.
[17] S. Solé, F. P. Gabbaï, *Chem. Commun.* **2004**, 1284–1285.
[18] V. C. Williams, W. E. Piers, W. Clegg, M. R. J. Elsegood, S. Collins, T. B. Marder, *J. Am. Chem. Soc.* **1999**, *121*, 3244–3245.
[19] Z. Q. Liu, M. Shi, F. Y. Li, Q. Fang, Z. H. Chen, T. Yi, C. H. Huang, *Org. Lett.* **2005**, *7*, 5481–5484.
[20] P. Anzenbacher Jr, K. Jursíková, J. L. Sessler, *J. Am. Chem. Soc.* **2000**, *122*, 9350–9351.
[21] H. Miyaji, W. Sato, J. L. Sessler, V. M. Lynch, *Tetrahedron Lett.* **2000**, *41*, 1369–1373.
[22] H. Yamamoto, A. Ori, K. Ueda, C. Dusemund, S. Shinkai, *Chem. Commun.* **1996**, 407–408.

[23] J. S. Wu, J. H. Zhou, P. F. Wang, X. H. Zhang, S. K. Wu, *Org. Lett.* **2005**, *7*, 2133–2136.
[24] S. Arimori, M. G. Davidson, T. M. Fyles, T. G. Hibbert, T. D. James, G. I. Kociok-Kohn, *Chem. Commun.* **2004**, *14*, 1640–1641.
[25] G. X. Xu, M. A. Tarr, *Chem. Commun.* **2004**, *9*, 1050–1051.
[26] C. R. Copper, N. Spencer, T. D. James, *Chem. Commun.* **1998**, 1365–1366.
[27] C. Dusemund, K. R. A. S. Sandanayake, S. J. Shinkai, *J. Chem. Soc., Chem. Commun. Chem. Soc., Chem. Commun.* **1995**, 333–334.
[28] H. Miyaji, W. Sato, J. L. Sessler, *Angew. Chem. Int. Ed.* **2000**, *39*, 1777–1780.
[29] S. Xu, K. C. Chen, H. Tian, *J. Mater. Chem.* **2005**, *15*, 2676–2680.
[30] C. J. Ward, P. Patel, T. D. James, *Chem. Lett.* **2001**, 406–407.
[31] A. B. Descalzo, D. Jiménez, J. El Haskouri, D. Beltrán, P. Amorós, M. D. Marcos, R. Martínez-Máñez, J. Soto, *Chem. Commun.* **2002**, 562–563.
[32] T. Gunnlaugsson, D. A. Mac Donaill, D. Parker, *J. Am. Chem. Soc.* **2001**, *123*, 12866–12876.
[33] S. Torelli, D. Imbert, M. Cantuel, G. Bernardinelli, S. Delahaye, A. Hauser, J.-C. G. Bünzli, C. Piguet, *Chem. Eur. J.* **2005**, *11*, 3228–3242.
[34] J. Zhang, P. D. Badger, S. J. Geib, S. Petoud, *Angew. Chem. Int. Ed.* **2005**, *44*, 2508–2512.
[35] H. Tsukube, S. Shinoda, *Chem. Rev.* **2002**, *102*, 2389–2404.
[36] J. C. G. Bünzli, *In Lanthanide Probes in Life, Chemical and Earth Sciences* (Eds.: J. C. G. Bünzli, G. R. Choppin), Elsevier, Amsterdam, **1989**.
[37] C. H. Huang (Ed.), *Chemistry of Rare Earth Complexes*, Science Press, Beijing, **1997**.
[38] I. A. Hemmila (Ed.), *Applications of Fluorescence in Immunoassays*, Wiley, New York, **1991**.
[39] J. Wang, R. Wang, J. Yang, Z. Zheng, M. D. Carducci, T. Cayon, N. Peyghambarian, G. E. Jabbour, *J. Am. Chem. Soc.* **2001**, *123*, 6179–6180.
[40] S. F. Li, G. Y. Zhong, W. H. Zhu, F. Y. Li, J. F. Pan, W. Huang, H. Tian, *J. Mater. Chem.* **2005**, *15*, 3221–3228.
[41] J. Kido, Y. Okamoto, *Chem. Rev.* **2002**, *102*, 2357–2368.
[42] M. Shi, F. Y. Li, T. Yi, D. Q. Zhang, H. M. Hu, C. H. Huang, *Inorg. Chem.* **2005**, *44*, 8929–8936.
[43] D. Parker, *Coord. Chem. Rev.* **2000**, *205*, 109–130.
[44] H. Shinoda, H. Tamiaki, *Coord. Chem. Rev.* **2002**, *226*, 227–234.
[45] T. Gunnlaugsson, J. P. Leonard, *Chem. Commun.* **2005**, 3114–3131.
[46] D. Parker, J. H. Yu, *Chem. Commun.* **2005**, 3141–3143.
[47] R. K. Mahajan, I. Kaur, R. Kaur, S. Uchida, A. Onimaru, S. Shinoda, H. Tsukube, *Chem. Commun.* **2003**, 2238–2239.
[48] K. Hanaoka, K. Kikuchi, H. Kojima, Y. Urano, T. Nagano, *J. Am. Chem. Soc.* **2004**, *126*, 12470–12476.
[49] L. J. Charbonnière, R. Ziessel, M. Montalti, L. Prodi, N. Zaccheroni, C. Boehme, G. Wipff, *J. Am. Chem. Soc.* **2002**, *124*, 7779–7788.
[50] M. Montalti, L. Prodi, N. Zaccheroni, L. Charbonnière, L. Douce, R. Ziessel, *J. Am. Chem. Soc.* **2001**, *123*, 12694–12695.
[51] N. Sabbatini, S. Perathoner, G. Lattanzi, S. Dellonte, V. Balzani, *J. Phys. Chem.* **1987**, *91*, 6136–6139.
[52] J. P. Cross, A. Dadabhoy, P. G. Sammes, *J. Lumin.* **2004**, *110*, 113–124.
[53] B. G. Huth, G. I. Farmer, M. R. Kagan, *J. Appl. Phys.* **1969**, *40*, 5145–5147.
[54] M. Xiao, P. R. Selvin, *J. Am. Chem. Soc.* **2001**, *123*, 7067–7073.
[55] M. Tanaka, G. Yamagughi, J. Shiokawa, C. Yamanaka, *B Chem. Soc. Jpn.* **1970**, *43*, 549–550.
[56] A. V. Hayes, H. G. Drickamer, *J. Chem. Phys.* **1982**, *76*, 114–125.
[57] F. J. Steemers, W. Verboom, D. N. Reinhoudt, E. B. van der Tol, J. W. Verhoeven, *J. Am. Chem. Soc.* **1995**, *117*, 9408–9414.
[58] M. Latva, H. Takalo, V. M. Mukkala, C. Matachescu, J. C. Rodriguez-Ubis, J. Kankare, *J. Lumin.* **1997**, *75*, 149–169.
[59] S. I. Klink, L. Grave, D. N. Reinhoudt, F. C. J. M. van Veggel, *J. Phys. Chem. A* **2000**, *104*, 5457–5468.
[60] J. Burgess, J. Kijowski, *Advances in Inorganic Chemistry and Radiochemistry*, Academic Press, **1981**.
[61] X. H. Zou, B. H. Ye, H. Li, J. G. Liu, Y. Xiong, L. N. Ji, *J. Chem. Soc., Dalton Trans.* **1999**, 1423–1428.
[62] H. Xin, M. Shi, X. C. Gao, Y. Y. Huang, Z. L. Gong, D. B. Nie, H. Cao, Z. Q. Bian, F. Y. Li, C. H. Huang, *J. Phys. Chem. B* **2004**, *108*, 10796–10800.
[63] P. P. Sun, J. P. Duan, J. J. Lih, C. H. Cheng, *Adv. Funct. Mater.* **2003**, *13*, 683–691.
[64] H. Xin, F. Y. Li, M. Shi, Z. Q. Bian, C. H. Huang, *J. Am. Chem. Soc.* **2003**, *125*, 7166–7167.
[65] G. M. Sheldrick, *SHELXTL-Plus V5.1 Software Reference Manual*, Bruker AXS Inc., Madison, WI, **1997**.

Received: November 29, 2005
Published Online: March 30, 2006

